Final Report

Enhanced Stability, Solubility and Anticancer Activity of Mansonones by Complexation with Cyclodextrins

By Thanyada Rungrotmongkol

March 2019

Contract No. RSA5980069

Final Report

Enhanced Stability, Solubility and Anticancer Activity of Mansonones by Complexation with Cyclodextrins

Researcher **Institute**

Asst. Prof. Dr. Thanyada Rungrotmongkol **Chulalongkorn University**

This project granted by the Thailand Research Fund

Project Code: RSA5980069

Project Title : Enhanced Stability, Solubility and Anticancer Activity of Mansonones by Complexation with Cyclodextrins

Investigator : Asst. Prof. Dr. Thanyada Rungrotmongkol

E-mail Address : thanyada.r@chula.ac.th, t.rungrotmongkol@gmail.com

Project Period: 3 years (July 1, 2015 – April 30, 2018)

Abstract:

DNA topoisomerase II catalyzes the changes in DNA structure by cleaving and rejoining one strand of the double stranded DNA. Due to their importance in several vital cell processes, topoisomerase II is one of the popular targets for design and development of newly potent anticancer drugs. Mansonones can be extracted from *Mansonia gagei* Drumm, a traditional medicinal plant in the *Sterculiaceae* family in Thailand, and many isolated and synthesized mansonones have shown the cytotoxicity towards various human cancer cell lines. Chalcones, the extracted compounds from several plants such as *Piper methysticum* or Angelica, showed the highly cytotoxicity against urinary bladder, cervical and breast cancer and exhibited an inhibitory activity towards DNA topoisomerase IIα. Herein, mansonones and chalcones against DNA topoisomerase were successfully screened by in silico and in vitro studies. However, mansonones show relatively low solubility and low physicochemical stability, leading to difficulties in pharmaceutical and biomedical applications. Solubility of mansonones was improved by complexation with cyclodextrins. In addition to the pharmaceutical and biomedical benefits, the results of this research would increase the values of mansonones, chalcones and cyclodextrins which are rich natural resources in Thailand with a consequence of local economy development.

Final report content:

1. Abstract

In Thai:

ดีเอ็นเอโทโปไอโซเมอเรส II เป็นเอนไซม์ที่เร่งปฏิกิริยาการคลายเกลียวสายเดี่ยวหรือสายคู่ของ DNA เนื่องจากเอนไซม์ดีเอ็นเอโทโปไอโซเมอเรส II มีความบทบาทสำคัญต่อกระบวนการแบ่งเซลล์ จึงทำให้เอนไซม์ดังกล่าวเป็นหนึ่งในโปรตีนเป้าหมายเพื่อใช้ในการออกแบบและพัฒนาสารต้านมะเร็งใหม่ๆ สารแมนโซโนนเป็นสารทางธรรมชาติที่สกัดจากแก่นไม้ของต้นจันทน์ชะมด (*Mansonia gagei* Drumm) ซึ่งเป็นพืชสมุนไพรไทยที่ใช้ทางการแพทย์ตระกูล Sterculiaceae จากงานวิจัยพบว่าทั้งสารสกัดและสารสังเคราะห์แมนโซโนนมีฤทธิ์ต้านมะเร็งได้หลากหลายชนิด ชาลโคนเป็นสารทางธรรมชาติที่สามารถสกัดได้จากพืชหลายชนิด ตัวอย่างเช่น Piper methysticum หรือ Angelica ซึ่งจากการศึกษาพบว่าสารกลุ่มนี้มีฤทธิ์ต้านมะเร็งปัสสาวะ มะเร็งปากมดลูกและมะเร็งเต้านมได้ดียิ่ง อีกทั้งยังมีฤทธิ์ยับยั้งเอนไซม์โทโปไอโซเมอร์เรส IIα จากการศึกษานี้โดยเทคนิคทางคอมพิวเตอร์และในหลอดทดลองพบว่าทั้งสารแมนโซโนนและสารชาลโคนสามารถยับยั้งเอนไซม์โทโปไอโซเมอร์เรส IIα อย่างไรก็ตามสารแมนโซโนนมีค่าการละลายน้ำและความเสถียรต่ำ ซึ่งเป็นอุปสรรคต่อการนำไปประยุกต์ใช้ด้านเภสัชกรรมและชีวการแพทย์ต่อไป ดังนั้นการสร้างสารประกอบเชิงซ้อนกับไซโคลเด็กทรินจึงเป็นทางเลือกหนึ่งที่สามารถเพิ่มค่าการละลายน้ำของสารแมนโซโนนได้ ผลการทดลองจากงานวิจัยนี้สามารถเพิ่มมูลค่าของสารแมนโซโนนชาลโคนและไซโคลเด็กทรินซึ่งเป็นผลิตภัณฑ์ที่สกัดจากสมุนไพรไทย และสามารถนำไปต่อยอดการได้ในอนาคต

In English:

DNA topoisomerase II catalyzes the changes in DNA structure by cleaving and rejoining one strand of the double stranded DNA. Due to their importance in several vital cell processes, topoisomerase II is one of the popular targets for design and development of newly potent anticancer drugs. Mansonones can be extracted from *Mansonia gagei Drumm*, a traditional medicinal plant in the *Sterculiaceae* family in Thailand, and many isolated and synthesized mansonones have shown the cytotoxicity towards various human cancer cell lines. Chalcones, the extracted compounds from several plants such as *Piper methysticum* or *Angelica*, showed the highly cytotoxicity against urinary bladder, cervical and breast cancer and exhibited an inhibitory activity towards DNA topoisomerase IIα. Herein, mansonones and chalcones against DNA topoisomerase were successfully screened by *in silico* and *in vitro* studies. However, mansonones show relatively low solubility and low physicochemical

stability, leading to difficulties in pharmaceutical and biomedical applications. Solubility of mansonones was improved by complexation with cyclodextrins. In addition to the pharmaceutical and biomedical benefits, the results of this research would increase the values of mansonones, chalcones and cyclodextrins which are rich natural resources in Thailand with a consequence of local economy development.

2. Executive Summary

Main findings of publications generated from this RSA grants are given as follows:

Project 1: *In silico screening of mansonones against DNA topoisomerase IIα*

The two molecular docking approaches suggested that mansonone derivatives (MGs) preferentially target to the ATPase domain of DNA topoisomerase IIα (TopoIIα) rather than to the etoposide pocket and the central domain. The eight potent MGs with higher binding affinities than that of salvicine, an ATP-competitive inhibitor, were selected for MD simulations and binding free energy calculations based on MM/PB(GB)SA methods. According to per-residue decomposition free energy analysis, the residues 87-88, 91-92, 94-95, 98-99, 125, 141-142, 147, 150, 161-162, 164-168, 215, and 217 were associated with ligand binding, by which van der Waals interactions mainly contributed for protein-ligand complexation rather than electrostatic forces and H-bond formations. Both MM/PB(GB)SA binding free energies showed that MG12, MG14, and MG15 exhibited the greater binding affinities with low solvent accessibility than those of salvicine and 1,4-BQ. Accordingly, the C-6 to C-10 lengths were suitable for aliphatic carbon sidechain of MG, whereas the C-12 length might cause the steric effect within ATP-binding pocket. Moreover, the ligand binding affected the secondary structures of TopoIIα for both inside and outside ATP-binding pocket. Especially, the binding of the most predicted potent compound MG14 promoted the conformational change of the turn structure (residues 145-151 of chain A) to become significantly located closer to the ligand and Mg^{2+}. Thus, this occurrence could be one of the crucial mechanisms underlying TopoIIα inhibition for this naphthoquinone-containing compound against ATPase domain of TopoIIα. Taken together, these theoretical calculations can provide useful structural information in terms of: *(i)* the suitable

length of carbon sidechain and/or aromatic moiety for the predictably potent MGs, *(ii)* binding orientation of ligands, and *(iii)* key amino acids involved in ligand binding, for further design and development of new targeted drugs containing naphthoquinone core against TopoIIα.

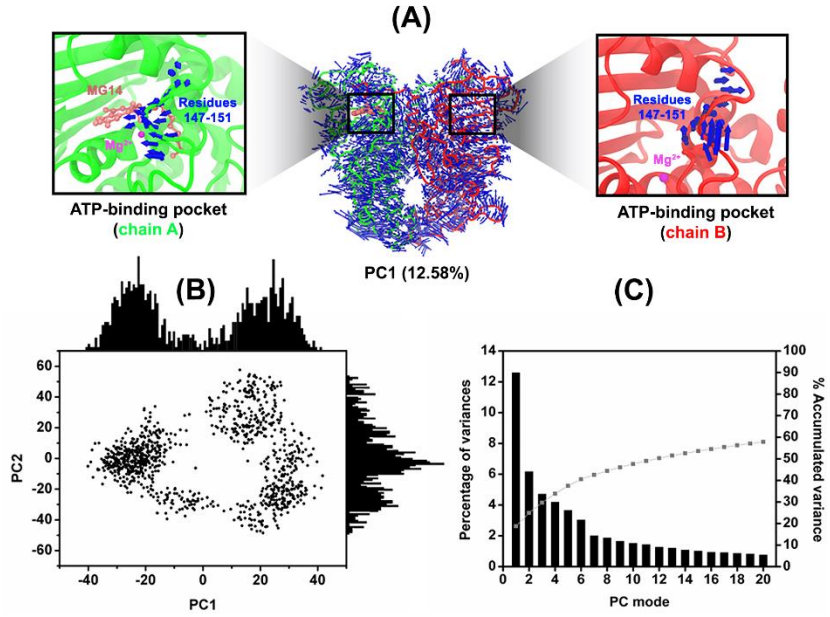

Figure 1. (**A**) Porcupine plot of MG14/TopoIIα complex showing the significant motion, especially turn region (residues 145-151). (**B**) The 2D projection of MD trajectories on the first two PCs. (**C**) PCA scree plot of quantitative characters.

Project 2: *In silico and in vitro screening of* chalcones *against DNA topoisomerase IIα*

Targeted cancer therapy has become one of the high potential cancer treatments. Human topoisomerase II (hTopoII), which catalyzes the cleavage and rejoining of double-stranded DNA, is an important molecular target for the development of novel cancer therapeutics. In order to diversify the pharmacological activity of chalcones and to extend the scaffold of topoisomerase inhibitors, a series of chalcones were screened against hTopoIIα by computational techniques, and subsequently tested for their cytotoxicity. From the

experimental IC_{50} values, chalcone **3d** showed a high cytotoxicity with IC_{50} values of 10.8, 3.2 and 21.1 μM against the HT-1376, HeLa and MCF-7 cancer-derived cell lines, respectively, and also exhibited an inhibitory activity against hTopoIIα-ATPase that was better than the known inhibitor, salvicine. The observed ligand-protein interactions from a molecular dynamics study affirmed that **3d** strongly interacts with the ATP binding pocket residues. Altogether, the newly synthesized chalcone **3d** has a high potential to serve as a lead compound for topoisomerase inhibitors.

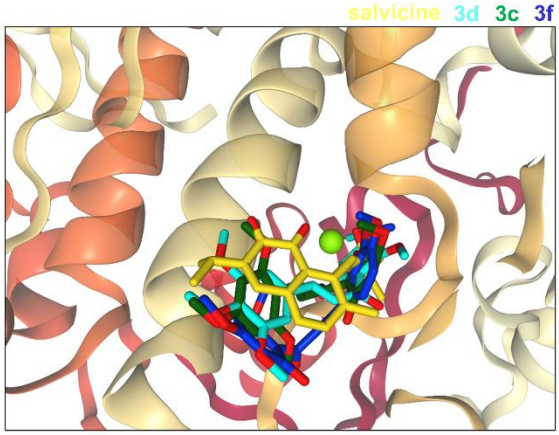

Figure 2. Superimposed structures of the three most active chalcones (**3c**, **3d** and **3f**) from the docking study with that of salvicine in the ATP-binding pocket of the hTopoIIα ATPase domain.

Project 3: *Formation of mansonone/cyclodextrin complex*

From MD simulation, mansonone molecules are able to form inclusion complexes quite well and that they are mostly positioned nearby the secondary rim of β-cyclodextrin (βCD) due to the effect of steric hindrance, which was supported by the highest amount of *n(r)* values of the unmodified βCD from RDF calculations. On the other hand, when the height of cavity was significantly increased in hydroxypropylated βCDs (i.e., 2,6-DHPβCD and 2-HPβCD), such steric hindrance was diminished and the ligands could slightly move down to the center of cavity coupled with the reduction of *n(r)* values of water accessibility. The PES calculation showed that the ligand binding affected the conformational changes of βCDs by

inducing the intramolecular hydrogen bond formation within the inclusion complexes to the most stable form. From the structural parameters of the angle analysis, the no-flip conformation was found to be the major population rather than one- or two-flip conformations of glucopyranose units, resulting from the small fluctuation occurred in the simulation. According to the MM-PBSA binding free energy calculation, as expected for encapsulating the lipophilic guest molecules into the hydrophobic inner cavities, van der Waals interaction was the main driving force for the complexation process rather than long-range electrostatic interactions. The inclusion complexes of mansonones with hydroxypropylated βCD derivative have a higher stability, and are suitable for inclusion complex formation. Moreover, the obtained free energies can provide the effect of enantioselectivity of βCD derivatives toward ME and MH enantiomers for further use in analytical techniques and pharmaceutical applications.

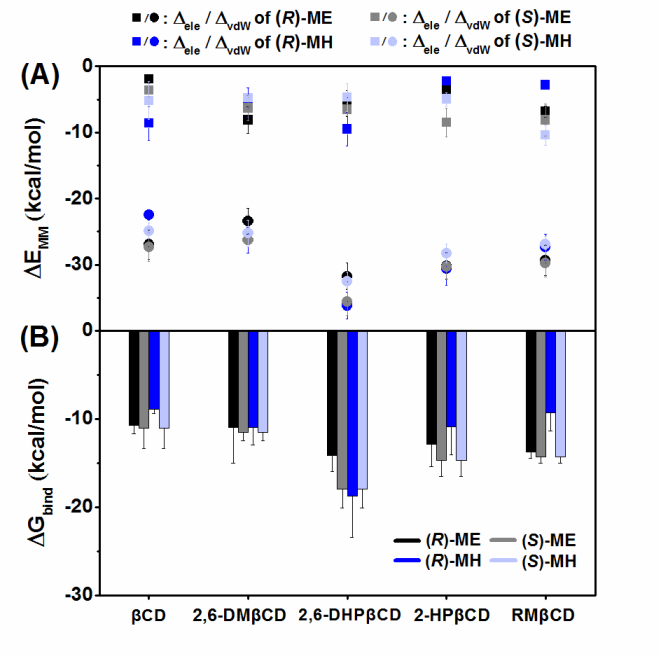

Figure 3. (**A**) Molecular mechanics energy components in gas phase and (**B**) the MM-PBSA binding free energy (ΔG_{bind}) for all simulated systems.

Project 4: *Conformations of 2-Hydroxypropyl-β-cyclodextrin*

2-Hydroxypropyl-β-cyclodextrin (HPβCD) has unique properties to enhance the stability and the solubility of low water-soluble compounds by inclusion complexation. An understanding of the structural properties of HPβCD and its derivatives, based on the number of 2-hydroxypropyl (HP) substituents at the α-D-glucopyranose subunits is rather important. In this work, replica exchange molecular dynamics simulations were performed to investigate the conformational changes of single and double-sided HP-substitution, called 6-HPβCDs and 2,6-HPβCDs, respectively. The results show that the glucose subunits in both 6-HPβCDs and 2,6-HPβCDs have a lower chance of flipping than in βCD. Also, HP groups occasionally block the hydrophobic cavity of HPβCDs, thus hindering drug inclusion. We found that HPβCDs with a high number of HP-substitutions are more likely to be blocked, while HPβCDs with double-sided HP-substitutions have an even higher probability of being blocked. Overall, 6-HPβCDs with three and four HP-substitutions are highlighted as the most suitable structures for guest encapsulation (Figure 4), based on our conformational analyses, such as structural distortion, the radius of gyration, circularity, and cavity self-closure of the HPβCDs.

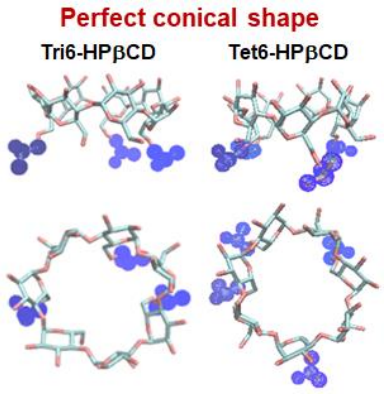

Figure 4. The perfect conical shape of 6-HPβCDs with three and four HP-substitutions, called as Tri6-HPβCDs and Tet6-HPβCDs

3. Objectives (there are four projects according to the summary mentioned above)

Project 1: *In silico screening of mansonones against DNA topoisomerase IIα*

The main bioactive MG extracted from Mansonia gagei and its semi-synthetic compounds were selected to study the preferential binding site and dynamics behavior as well as to predict the inhibitory activity against TopoIIα using molecular modeling techniques.

Project 2: *In silico and in vitro screening of* chalcones *against DNA topoisomerase IIα*

In order to find new potential anti-cancer agents against hTopoIIα, the newly 47 chalcone derivatives were designed and then screened in silico using a molecular docking approach. The potent chalcones with a more favorable interaction energy than that of the known hTopoIIα inhibitors were then synthesized and tested for their *in vitro* cytotoxicity towards three cell lines derived from urinary bladder (HT-1376), cervical (HeLa) and breast (MCF-7) cancers. Then, all-atom molecular dynamics (MD) simulations were performed to investigate the structure and dynamics properties as well as the ligand-target interactions between the most potent chalcone and hTopoIIα.

Project 3: *Formation of mansonone/cyclodextrin complex*

Mansonone E (ME) and H (MH) enantiomers were subjected to investigate the structural dynamics as well as to predict the suitable host molecules for inclusion complexation using computational tools.

Project 4: *Conformations of 2-Hydroxypropyl-β-cyclodextrin*

We applied the replica exchange molecular dynamics (REMD) method on βCD and HPβCDs models to study the conformational change affected by the different numbers of HP-substitutions on the O2 and/or O6 atoms. The structural behaviors of all models were analyzed based on structural distortion analysis, the radius of gyration, circularity, and the cavity self-closure of the HPβCDs. By doing so, the best candidate of the HPβCDs with a suitable amount of HP-substitution, representing the perfect conical shape for molecular encapsulation, will be provided as a useful guideline for the suitable substitution degree of HPβCD.

Note: The outputs of the all objectives will be given in Appendix section

4. Methodology

Project 1: *In silico screening of mansonones against DNA topoisomerase IIα*

Preparation of initial structure and molecular docking

The crystal structure of human TopoIIα ATPase domain complexed with AMP-PNP (PDB ID: 1ZXM) [1] and cleavage/relegation domain complexed with DNA (PDB ID: 4FM9) [2] containing the merbarone binding pocket inside the central domain [3] were obtained from Protein Data Bank (PDB). To search for the etoposide binding pocket, a homology model of TopoIIα was constructed by SWISS-MODEL server [4] using etoposide-TopoIIβ complex (PDB ID: 3QX3) as a template according to the previous study [5]. Afterward, the homology model and template were superimposed to identify the location and amino acid residues of etoposide binding site (**Fig. S1 in supplementary data**). The protonation states of all ionizable amino acids were determined at pH 7.0 using PROPKA 3.0 [6]. The starting structures of salvicine (**14690081**), 1,4-BQ (**895247**), etoposide (**3938684**), and merbarone (**17128283**) were taken from ZINC database [7], whereas the MG and its 18 derivatives were built according to the previous research [8, 9] and fully optimized by the HF/6-31(d) level of theory using Gaussian09 program [10]. Subsequently, each of them was docked with 100 independent docking runs into three different pockets of TopoIIα using CDOCKER module [11] in the Accelrys Discovery Studio 2.5[Accelrys Inc.] and selective integrated tempering sampling based docking (SBD) approach [12]. Note that (*i*) the co-crystalized AMP-PNP (**Fig. 1B**), (*ii*) etoposide (**Fig. 1C**), and (*iii*) Mg^{2+} and TyrB805 (**Fig. 1D**) were defined as binding sites (CDOCKER: 15 Å of sphere radius and SBD: 22 x 18 x 20 Å of grid box) for ATPase domain, etoposide binding pocket, and central domain, respectively. According to the standard procedure [13-15], the electrostatic potential (ESP) charges around the optimized MG structures were computed using the same method and basis set. The antechamber and parmchk modules implemented in AMBER16 were used to generate the restrained ESP (RESP) charges and corresponding parameters of MGs, respectively. The AMBER ff14SB force field [16] was applied for the protein, whereas the ligands were treated by the generalized AMBER force field (GAFF) [17]. The missing hydrogen atoms were added by the LEaP module followed by minimization with 1000 steps of the steepest descents (SD) and continued by 2500 steps of conjugated gradient (CG) approaches on the hydrogen atoms only. Afterward, each system was solvated using TIP3P water model [18] in truncated octahedron periodic box with the minimum distance of 12 Å from the protein surface. The chloride ions were added for neutralizing the systems. The water molecules only were then

minimized using the same SD and CG minimization processes. Lastly, the whole system was fully minimized using the same procedures.

Selective integrated tempering sampling (SITS) based docking

Selective integrated tempering sampling (SITS) is the technique that can selectively enhance the sampling of the solute without transforming the solvent structures [12]. This method combines the replica exchange with solute tempering (REST) [19, 20] with integrated tempering enhanced sampling (ITS) simulations [21].

Molecular dynamics simulations and free energy calculations

The selected enzyme-ligand complexes from molecular docking were subsequently studied by MD simulations under periodic boundary condition with *NPT* ensemble using time steps of 2 fs according to previous works [22-24]. The Particle Mesh Ewald (PME) summation approach was applied to treat long-range electrostatic interactions [25], whereas the short-range cutoff for non-bonded interactions was set as 12 Å. Temperature and pressure were controlled by Berendsen weak coupling algorithm [26]. The SHAKE algorithm was used to constrain all covalent bonds involving hydrogen atoms [27]. The simulated models were heated up to 310 K for 100 ps and continuously held at this temperature for another 80 ns. The root-mean-square displacement (RMSD), hydrogen bond (H-bond) occupation, solvent accessible surface area (SASA), and principal component analysis (PCA) were calculated by the cpptraj module, whereas the MM/PB(GB)SA binding free energy and the per-residue decomposition energy were estimated by MM/PBSA.py implemented in AMBER16.

Project 2: *In silico and in vitro screening of* chalcones *against DNA topoisomerase IIα*

Computational methods

Molecular docking

Due to the possibility of the inhibition of two motifs of the hTopoIIα (ATP binding site in the ATPase domain and the etoposide binding pocket in the hTopoIIα/DNA complex), the predicting mode of the inhibitory activity of chalcones on both sites was studied by molecular docking using the CDOCKER module of Accelrys Discovery Studio 3.0 (Accelrys, Inc.) as previously reported [28]. The starting structures of the 47 designed chalcone derivatives were built by the GaussView program, while those of salvicine and etoposide were taken from the ZINC database. To validate the docking method, the co-crystallized ligands were initially docked into the

binding pocket with 100 independent runs, i.e., docking of AMP-PNP into the ATP binding site of the hTopoIIα ATPase domain (1ZXM.pdb), and etoposide into its binding pocket of the hTopoIIα/DNA complex (3QX3.pdb). The position of docked ligands did not differ significantly from the crystallized conformation ligands (RMSD = 0.80 Å for AMP-PNP and 0.44 Å for etoposide) and so the 47 chalcones were then separately docked into both sites, while salvicine (used as the reference compound at the ATPase domain) was only docked into the ATP binding site. The chalcones with predicted interaction energies towards hTopoIIα that were more favorable than those of the known inhibitors were synthesized and their cytotoxicity against the three cancer cell lines was tested.

MD simulation

All-atom MD simulations under a periodic boundary condition were performed on the most potent chalcone selected from the in vitro cytotoxicity study (section 2.3.3) in complex with hTopoIIα in aqueous solution, following the previously reported MD study on the binding of mansonone G to hTopoIIα [28]. The partial charges of the ligand were prepared according to standard procedures [23]. The ligand was optimized with ab initio calculation using the HF/6-31G* method in the Gaussian09 program [29]. The electrostatic potential (ESP) charges of the ligand were calculated using the same level of theory, and then the restrained ESP (RESP) charges were obtained by the charge fitting procedure using the antechamber module in the AMBER 14 package program [30]. The general AMBER force field (GAFF) and AMBER ff03 force field [31] were applied for the ligand and protein, respectively. The protonation states of all ionizable amino acids were determined using PROPKA 3.1[32]. The complex was solvated by TIP3P water molecules [18] within 12 Å around the system surface. Chloride ions were introduced to neutralize the total positive charge of the chalcone/hTopoIIα complex.

To remove the bad contacts and steric hindrance, the added hydrogen atoms were minimized with 1000 steps of steepest descents (SD) followed by 2000 steps of conjugated gradients (CG) using the Sander module in AMBER 14. The water molecules and ions were then minimized with 500 steps of SD followed by 500 steps of CG, while a 500 kcal/mol $Å^2$ force constant was used to restrain hTopoIIα. The whole system was then fully

minimized with 1000 steps of SD and CG. All covalent bonds involving hydrogen atoms were constrained by the SHAKE algorithm [33]. The long-range electrostatic interactions were calculated according to the Particle Mesh Ewald (PME) approach [25] with a cutoff distance of 12 Å for non-bonded interactions.

The system was heated to 310 K for 100 ps and then simulated at the same temperature for 80 ns in the NPT ensemble using a time step of 2 fs. The MD trajectories in the production phase were taken for analysis in terms of the per-residue decomposition free energy and intermolecular hydrogen bonds (H-bonds) between the ligand and hTopoIIα using the MM/PBSA.py and cpptraj modules, respectively. The percentage of H-bond occupation was calculated using the two criteria of: (i) the distance between proton donor (HD) and acceptor (HA) atoms $\leq$ 3.5 Å, and (ii) the angle of HD-H…HA > 120°.

Experimental approach

Synthesis of chalcone derivatives

The three selected chalcones (**3c**, **3d** and **3f**) were synthesized by Claisen-Schmidt condensation with some modifications between selected acetophenones and benzaldehydes under a basic condition, according to the procedures described by Cabrera [34]. The target products were purified by column chromatography and their structures were elucidated by NMR spectroscopy.

Cell culture and sample preparation

Stock cultures of HT-1376, HeLa and MCF-7 cell lines were grown in T-75 flasks in complete medium (CM; DMEM, 10% (v/v) FBS and 1% (v/v) Pen-Strep) at 37 °C under 5% (v/v) CO_2. They were subculture once a week, for HeLa and MCF-7 cells at a 1:100 ratio and for HT-1376 at 1:20 ratio by washing with PBS and then the cells were detached with trypsin. The 10^{-1} M stock solution of each respective chalcone derivative was prepared in 100% DMSO.

Cytotoxicity assay

The cytotoxicity of the chalcones and salvicine was measured according to a published method [35] with some modifications. The cell viabilities of three cancer cell lines (HT-1376, HeLa and MCF-7) exposed to the

screened chalcone derivatives were evaluated by the MTT assay. The cell suspension (100 μL) was seeded into 96-well plates at a density of 2 × 10^6 cells/well and then incubated for 24 h under normal culture conditions before the addition of the respective test compound at various concentrations (100, 50, 25, 12.5 and 0 (control) μM and incubated for another 24 h. Then, 10 μL of fresh MTT solution (5 mg/mL) was added to each well and incubated at 37 °C for 2 h, before the reaction was stopped by adding 100 μL of DMSO. The absorbance was measured at 570 nm with correction for background at 690 nm using a microplate spectrophotometer system (Infinite M200 micro-plate reader, Tecan). The amount of the colored product is assumed to be directly proportional to the number of viable cells. Each experiment was performed in triplicate and repeated three times. The percentage cell viability in each compound was calculated relative to the control, and the IC_{50} values were determined in comparison with untreated controls using the Table Curve 2D program version 5.01.

Expression and enrichment of the recombinant (*r*)hTopoIIα ATPase domain

Expression and enrichment of the *r*hTopoIIα ATPase domain was modified from that reported [36]. The expression plasmid pET28b-hTopoIIα-ATPase was transformed into Escherichia coli BL21 (DE3) cells and a transformant colony was selected for large-scale protein expression and grown at 37°C to an optical density at 600 nm of ~0.6 in LB broth (2 L) containing 50 μg/mL kanamycin. Protein expression was then induced by adding 0.5 mM IPTG at 30 °C for 5 h. The cells were harvested by centrifugation at 6000x g, 4°C and resuspended in lysis buffer (50 mM Tris-Cl pH.8, 0.5 M NaCl, 5 mM imidazole, 0.5% (v/v) TritonX-100, 1 mM PMSF) and lysed by sonication. After clarification by centrifugation (as above) the supernatant was harvested, and the *r*hTopoIIα-ATPase enriched for using HisTrap Chelating HP and Resource S column chromatography, eluting in exchange buffer (50 mM Tris pH.7.5, 50 mM NaCl, 5% (v/v) glycerol, 50 mM KCl, 5 mM $MgCl_2$) from a PD-10 desalting column. The enriched protein was analyzed by 12% sodium dodecyl sulphate-polyacrylamide gel electrophoresis (SDS-PAGE) and stained by Coomassie blue.

ATPase assay

The inhibitory activities of salvicine and chalcone **3d** were determined by measuring the ATPase activity of rhTopoIIα-ATPase using the ADP-Glo™ Kinase Assay. Briefly, 8 μL of buffer (40 mM Tris-HCl pH 7.5, 20 mM MgCl2, 0.1 mg/mL BSA) was added to each well of a 384-well plate (Promega, solid white) with 5 μL of enzymes (10 ng/μL) and 2 μL of the test compound at different concentrations. The reaction was initiated by the addition of 5 μL of 12.5 μM ATP, allowed to proceed for 1 h at room temperature and then stopped by the addition of 5 μL of ADP-Glo™ Reagent and incubating at room temperature for 40 min. Next, 10 μL of Detection Reagent was added and incubated for 30 min prior to the addition of luciferase and luciferin to detect the ATP by measuring the luminescence of each well with a microplate spectrophotometer system (Synergy HTX Multi-Mode reader, BioTek). All assays were performed in triplicate.

Project 3: *Formation of mansonone/cyclodextrin complex*

The optimized structures of βCD and its four derivatives (2,6-DMβCD, 2-HPβCD, 6-HPβCD and 2,6-DHPβCD) were taken from our previous study [37]. Note that the commercially available HPβCD is a partially substituted poly(hydroxypropyl) ether of βCD with various degrees of substitution (DS) [38]. Three models of HPβCD derivatives including 2-HPβCD (DS=1), 6-HPβCD (DS=1) and 2,6-DHPβCD (DS=2) [39] were used as representative structures for the study of the encapsulation reaction. For the RMβCD, the structure was constructed by removing some substituents from 2,6-DMβCD according to the strength of nucleophilicity (primary hydroxyl groups > secondary hydroxyl groups). Therefore, the three methyl groups are located on the secondary rim at the D-(+)-glucopyranose units 1, 3 and 5, while the hydroxyl groups on the primary rim were fully substituted by seven methyl groups. The starting structures of two mansonones, ME and MH, including their stereoisomers were built and subsequently optimized by the HF/6-31(d) basis set using Gaussian09 program [29]. The inclusion complexes between each mansonone molecule and all six βCDs were constructed by a docking procedure with 500 independent runs using the CDOCKER module implemented in the Accelrys Discovery Studio 2.5[Accelrys Inc.]. Subsequently, the best three docked complexes at each binding mode were then

studied by the classical MD simulations in aqueous solutions using the AMBER14 software package [40]. According to the standard procedures [13, 41-43], the electrostatic potential (ESP) charges around the optimized mansonone structures were calculated by HF/6-31(d) level of theory using Gaussian09 program. The charge fitting procedure (antechamber module) and parmchk module were used for generating the restrained electrostatic potential (RESP) charges and their parameters of two mansonones, respectively. The Glycam06 force field [44] was applied for βCD and its derivatives, whereas the mansonones were treated by the generalized AMBER force field (GAFF). To release bad contacts and to relax the structures prior to MD simulations, all hydrogen atoms of βCDs and the mansonone molecules were minimized with 1000 steps of the steepest descents (SD) method and continued by 3000 steps of conjugated gradient (CG) method. Afterwards, the inclusion complexes were solvated using TIP3P water model with the minimum distance of 15 Å from the system surface. As a result, all systems consisted of 2100 ± 42 water molecules in an approximately 50 × 50 × 50 $Å^3$ truncated octahedron periodic box. The water molecules were then only minimized with the SD (1000 steps) and CG (3000 steps). Finally, the whole system was minimized using the same minimization process. The periodic boundary condition with *NPT* ensemble was applied for all simulated systems using a time step of 2 fs. Pressure and temperature were controlled by the Berendsen weak coupling algorithm [26]. The cutoff distance for long-range electrostatic interactions was set to 12 Å using the Particle Mesh Ewald (PME) summation approach [45]. The SHAKE algorithm [27] was used to constrain all bonds involving hydrogen atoms. The models were heated up to 298 K with the relaxation time of 60 ps, and continuously held at this temperature for another 30 ns. The cpptraj module of AMBER14 program was used to calculate the root-mean-square displacement (RMSD), the potential energy surface (PES), the flip angle of glucopyranose units, the distance between the centers of gravity of each mansonone ring and βCD(s), and the radial distribution function (RDF). The MM-PBSA binding free energy of all inclusion complexes were estimated by mm_pbsa.pl module [46] using the 100 snapshots extracted from the last 5-ns simulation.

Project 4: *Conformations of 2-Hydroxypropyl-β-cyclodextrin*

The optimized structures of native βCD and Hep6-HPβCD were taken from our previous studies [37, 47]]. The other HPβCD derivatives were prepared by different numbers of 2-hydroxypropyl (HP) substitutions at the O2 or O6 positions on α-D-glucopyranose units with substitution degrees of around 0.14–1.14 from one to eight HP-substitutions on βCD, as shown in Figure 4 The HP-substitutions on βCD in this work were divided into two groups, single- and double-sided substitutions. For the single-sided HP-substitution (Figure 4a), the HP groups were substituted with from one up to seven HP, only on O6 atoms of the primary rim (called as 6-HPβCDs), because the O6 is more reactive compared to O2 atoms of the secondary rim. In the case of double-sided HP-substitution (Figure 4b), the structures were generated by introducing from one up to four HP groups at the O2 atoms of the non-substituted glucose units (called as 2,6-HPβCD), as defined in Table 4

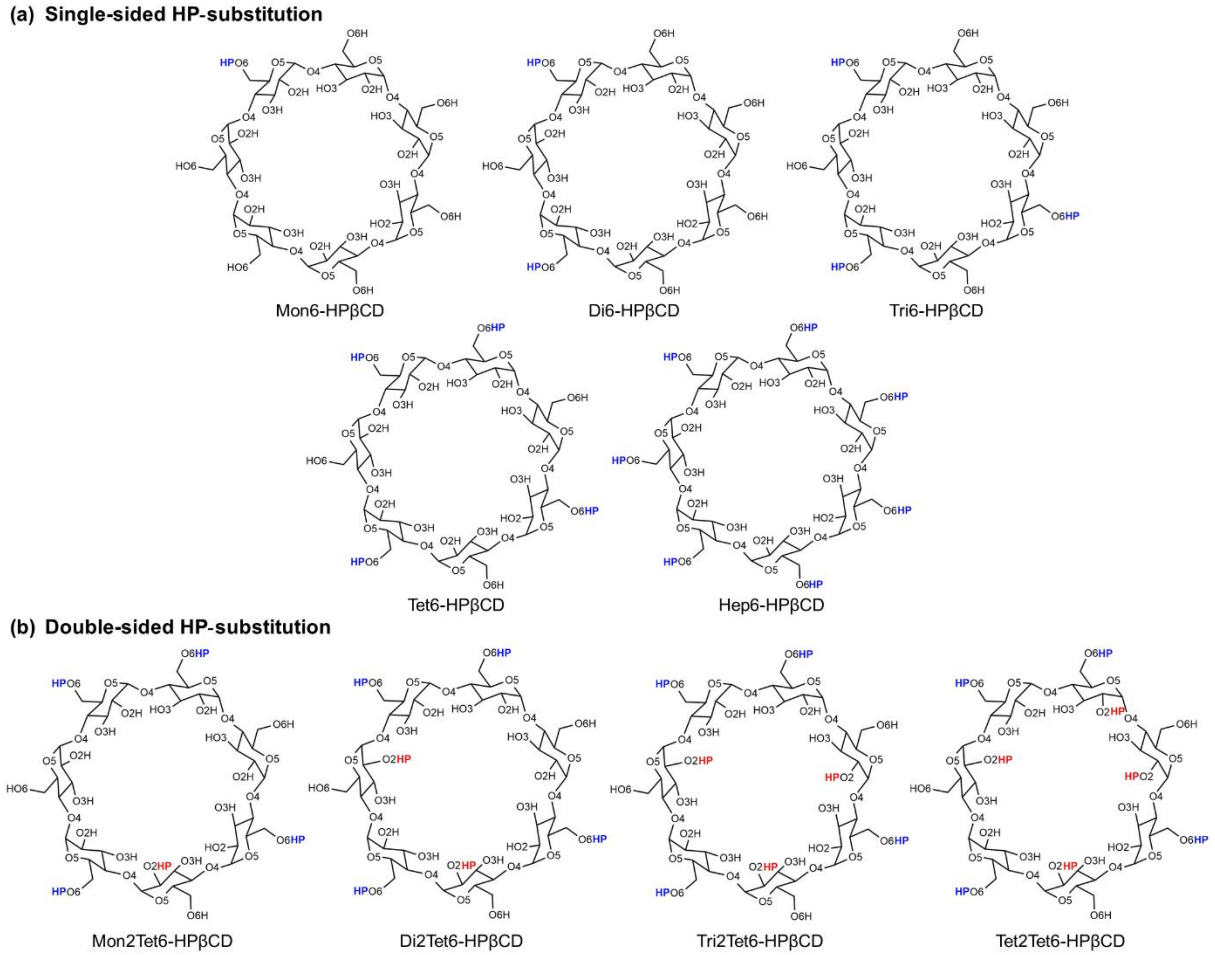

Figure 4. Models introducing 2-hydroxypropyl (HP) groups at the O2 (red) and/or O6 (blue) positions on glucose subunits.

Table 4. Model summary of introducing HP groups at the O2 and/or O6 positions on glucose subunits.

Models	Degree of Substitution	O2 Substitution	O6 Substitution
βCD	0.00	None	None
Single-sided HP-substitution			
Mon6-HPβCD	0.14	None	1 (At glucose unit 1)
Di6-HPβCD	0.28	None	2 (At glucose units 1 and 3)
Tri6-HPβCD	0.43	None	3 (At glucose units 1, 3, and 5)
Tet6-HPβCD	0.57	None	4 (At glucose units 1, 3, 5, and 7)
Hep6-HPβCD	1.00	None	7 (At all glucose units)
Double-sided HP-substitution			
Mon2Tet6-HPβCD	0.71	1 (At glucose unit 4)	4 (At glucose units 1, 3, 5, and 7)
Di2Tet6-HPβCD	0.85	2 (At glucose units 2 and 6)	4 (At glucose units 1, 3, 5, and 7)
Tri2Tet6-HPβCD	1.00	3 (At glucose units 2, 4, and 6)	4 (At glucose units 1, 3, 5, and 7)
Tet2Tet6-HPβCD	1.14	4 (At glucose units 2, 4, 6, and 7)	4 (At glucose units 1, 3, 5, and 7)

Overall, 10 CD structures were generated, to study how different numbers of HP influence the structural behavior, using REMD simulations. A detailed information of the REMD method is given elsewhere [48, 49]. The REMD simulations were performed by the Amber 14 package [50]. The parameters of βCD and HPβCDs were taken from the Glycam06 carbohydrate force field [51, 52], with the solvation model based on the generalized Born (GB) implicit solvent model, Igb5, which gives a suitable description of cyclodextrin εCD, as reported by Khuntawee et al. [53], and the smaller sizes of CDs (αCD-γCD, unpublished data) relative to the available crystal structures and MD studies in the explicit solvent model. The initial structures of βCD and all HPβCDs were fully minimized with 2000 steps of the steepest descent method, followed by 1000 steps of the conjugated gradient method to relax the structures before simulation. The REMD simulations were performed for 30 ns per replica, including an equilibration step for 5 ns, and the conformations at all temperatures were collected every 1 ps for 25 ns. The temperature distribution and the number of replicas were tested to obtain a reasonable replica exchange simulation. The results confirm that the temperature from 269.5 K to 570.9 K, with interval steps of around 30-60 K, was proper for the present case. All parameters of the structural distortion,

the radius of gyration, circularity, and cavity self-closure were analyzed from 25,000 snapshots taken from REMD simulations.

References

1. Wei, H., et al., *Nucleotide-dependent domain movement in the ATPase domain of a human type IIA DNA topoisomerase.* J Biol Chem, 2005. **280**(44): p. 37041-7.
2. Wendorff, T.J., et al., *The structure of DNA-bound human topoisomerase II alpha: conformational mechanisms for coordinating inter-subunit interactions with DNA cleavage.* J Mol Biol, 2012. **424**(3-4): p. 109-24.
3. Baviskar, A.T., et al., *Switch in Site of Inhibition: A Strategy for Structure-Based Discovery of Human Topoisomerase IIalpha Catalytic Inhibitors.* ACS Med Chem Lett, 2015. **6**(4): p. 481-5.
4. Schwede, T., et al., *SWISS-MODEL: an automated protein homology-modeling server.* Nucleic Acids Research, 2003. **31**(13): p. 3381-3385.
5. Drwal, M.N., et al., *Novel DNA Topoisomerase IIα Inhibitors from Combined Ligand- and Structure-Based Virtual Screening.* PLoS ONE, 2014. **9**(12): p. e114904.
6. Olsson, M.H., et al., *PROPKA3: Consistent Treatment of Internal and Surface Residues in Empirical pKa Predictions.* J Chem Theory Comput, 2011. **7**(2): p. 525-37.
7. Irwin, J.J., et al., *ZINC: A Free Tool to Discover Chemistry for Biology.* Journal of Chemical Information and Modeling, 2012. **52**(7): p. 1757-1768.
8. Hairani, R., R. Mongkol, and W. Chavasiri, *Allyl and prenyl ethers of mansonone G, new potential semisynthetic antibacterial agents.* Bioorg Med Chem Lett, 2016. **26**(21): p. 5300-5303.
9. Kim, H.K., et al., *CBMG, a novel derivative of mansonone G suppresses adipocyte differentiation via suppression of PPARγ activity.* Chemico-Biological Interactions, 2017. **273**: p. 160-170.
10. Frisch, M.J., et al., *Gaussian 09*. 2009, Gaussian, Inc.: Wallingford, CT, USA.
11. Wu, G., et al., *Detailed analysis of grid-based molecular docking: A case study of CDOCKER-A CHARMm-based MD docking algorithm.* J Comput Chem, 2003. **24**(13): p. 1549-62.
12. Yang, L. and Y. Qin Gao, *A selective integrated tempering method.* J Chem Phys, 2009. **131**(21): p. 214109.
13. Meeprasert, A., et al., *Binding pattern of the long acting neuraminidase inhibitor laninamivir towards influenza A subtypes H5N1 and pandemic H1N1.* J Mol Graph Model, 2012. **38**: p. 148-54.
14. Sangpheak, W., et al., *Enhanced stability of a naringenin/2,6-dimethyl beta-cyclodextrin inclusion complex: molecular dynamics and free energy calculations based on MM- and QM-PBSA/GBSA.* J Mol Graph Model, 2014. **50**: p. 10-5.
15. Nutho, B., et al., *Binding mode and free energy prediction of fisetin/β-cyclodextrin inclusion complexes.* Beilstein Journal of Organic Chemistry, 2014. **10**: p. 2789-2799.

16. Maier, J.A., et al., *ff14SB: Improving the Accuracy of Protein Side Chain and Backbone Parameters from ff99SB.* Journal of Chemical Theory and Computation, 2015. **11**(8): p. 3696-3713.
17. Wang, J., et al., *Development and testing of a general amber force field.* J Comput Chem, 2004. **25**(9): p. 1157-74.
18. Jorgensen, W.L., et al., *Comparison of simple potential functions for simulating liquid water.* The Journal of Chemical Physics, 1983. **79**(2): p. 926-935.
19. Liu, P., et al., *Replica exchange with solute tempering: A method for sampling biological systems in explicit water.* Proceedings of the National Academy of Sciences of the United States of America, 2005. **102**(39): p. 13749-13754.
20. Huang, X., et al., *Replica Exchange with Solute Tempering: Efficiency in Large Scale Systems.* The Journal of Physical Chemistry B, 2007. **111**(19): p. 5405-5410.
21. Gao, Y.Q., *An integrate-over-temperature approach for enhanced sampling.* J Chem Phys, 2008. **128**(6): p. 064105.
22. Meeprasert, A., S. Hannongbua, and T. Rungrotmongkol, *Key binding and susceptibility of NS3/4A serine protease inhibitors against hepatitis C virus.* J Chem Inf Model, 2014. **54**(4): p. 1208-17.
23. Kaiyawet, N., T. Rungrotmongkol, and S. Hannongbua, *Effect of Halogen Substitutions on dUMP to Stability of Thymidylate Synthase/dUMP/mTHF Ternary Complex Using Molecular Dynamics Simulation.* Journal of Chemical Information and Modeling, 2013. **53**(6): p. 1315-1323.
24. Phanich, J., et al., *A 3D-RISM/RISM study of the oseltamivir binding efficiency with the wild-type and resistance-associated mutant forms of the viral influenza B neuraminidase.* Protein Sci, 2016. **25**(1): p. 147-58.
25. York, D.M., T.A. Darden, and L.G. Pedersen, *The effect of long-range electrostatic interactions in simulations of macromolecular crystals: A comparison of the Ewald and truncated list methods.* The Journal of chemical physics, 1993. **99**(10): p. 8345-8348.
26. Berendsen, H.J.C., et al., *Molecular dynamics with coupling to an external bath.* The Journal of Chemical Physics, 1984. **81**(8): p. 3684-3690.
27. Ryckaert, J.-P., G. Ciccotti, and H.J.C. Berendsen, *Numerical integration of the cartesian equations of motion of a system with constraints: molecular dynamics of n-alkanes.* Journal of Computational Physics, 1977. **23**(3): p. 327-341.
28. Mahalapbutr, P., et al., *Molecular recognition of naphthoquinone-containing compounds against human DNA topoisomerase IIα ATPase domain: A molecular modeling study.* Journal of Molecular Liquids, 2017. **247**: p. 374-385.
29. Frisch, M.J., et al., *Gaussian 09, Revision B.01*. 2009: Wallingford CT.
30. D.A. Case, R.M.B., D.S. Cerutti, T.E. Cheatham, III, T.A. Darden, R.E. Duke, T.J. Giese, H. Gohlke, A.W. Goetz, N. Homeyer, S. Izadi, P. Janowski, J. Kaus, A. Kovalenko, T.S. Lee, S. LeGrand, P. Li, C. Lin, T. Luchko, R. Luo, B. Madej, D. Mermelstein, K.M. Merz, G. Monard, H. Nguyen, H.T. Nguyen, I.

Omelyan, A. Onufriev, D.R. Roe, A. Roitberg, C. Sagui, C.L. Simmerling, W.M. Botello-Smith, J. Swails, R.C. Walker, J. Wang, R.M. Wolf, X. Wu, L. Xiao and P.A. Kollman, *AMBER 2016.* University of California San Francisco, 2016.

31. Duan, Y., et al., *A point-charge force field for molecular mechanics simulations of proteins based on condensed-phase quantum mechanical calculations.* Journal of computational chemistry, 2003. **24**(16): p. 1999-2012.
32. Olsson, M.H., et al., *PROPKA3: consistent treatment of internal and surface residues in empirical p K a predictions.* Journal of chemical theory and computation, 2011. **7**(2): p. 525-537.
33. Ryckaert, J.-P., G. Ciccotti, and H.J. Berendsen, *Numerical integration of the cartesian equations of motion of a system with constraints: molecular dynamics of n-alkanes.* Journal of computational physics, 1977. **23**(3): p. 327-341.
34. Cabrera, M., et al., *Synthetic chalcones, flavanones, and flavones as antitumoral agents: Biological evaluation and structure–activity relationships.* Bioorganic & Medicinal Chemistry, 2007. **15**(10): p. 3356-3367.
35. Sangpheak, W., et al., *Physical properties and biological activities of hesperetin and naringenin in complex with methylated β-cyclodextrin.* Beilstein journal of organic chemistry, 2015. **11**(1): p. 2763-2773.
36. Boonyalai, N., et al., *Biophysical and molecular docking studies of naphthoquinone derivatives on the ATPase domain of human topoisomerase II.* Biomedicine & Pharmacotherapy, 2013. **67**(2): p. 122-128.
37. Kicuntod, J., et al., *Inclusion complexation of pinostrobin with various cyclodextrin derivatives.* J Mol Graph Model, 2016. **63**: p. 91-8.
38. Yuan, C., B. Liu, and H. Liu, *Characterization of hydroxypropyl-β-cyclodextrins with different substitution patterns via FTIR, GC–MS, and TG–DTA.* Carbohydrate Polymers, 2015. **118**: p. 36-40.
39. Wongpituk, P., et al., *Structural dynamics and binding free energy of neral-cyclodextrins inclusion complexes: molecular dynamics simulation.* Molecular Simulation, 2017: p. 1-8.
40. Walker, R.C., M.F. Crowley, and D.A. Case, *The implementation of a fast and accurate QM/MM potential method in Amber.* J Comput Chem, 2008. **29**(7): p. 1019-31.
41. Kaiyawet, N., T. Rungrotmongkol, and S. Hannongbua, *Effect of halogen substitutions on dUMP to stability of thymidylate synthase/dUMP/mTHF ternary complex using molecular dynamics simulation.* J Chem Inf Model, 2013. **53**(6): p. 1315-23.
42. Khuntawee, W., T. Rungrotmongkol, and S. Hannongbua, *Molecular dynamic behavior and binding affinity of flavonoid analogues to the cyclin dependent kinase 6/cyclin D complex.* J Chem Inf Model, 2012. **52**(1): p. 76-83.
43. Meeprasert, A., et al., *In silico screening for potent inhibitors against the NS3/4A protease of hepatitis C virus.* Curr Pharm Des, 2014. **20**(21): p. 3465-77.

44. Kirschner, K.N., et al., *GLYCAM06: a generalizable biomolecular force field. Carbohydrates.* J Comput Chem, 2008. **29**(4): p. 622-55.

45. Luty, B.A. and W.F. van Gunsteren, *Calculating Electrostatic Interactions Using the Particle−Particle Particle−Mesh Method with Nonperiodic Long-Range Interactions.* The Journal of Physical Chemistry, 1996. **100**(7): p. 2581-2587.

46. Rastelli, G., et al., *Fast and accurate predictions of binding free energies using MM-PBSA and MM-GBSA.* J Comput Chem, 2010. **31**(4): p. 797-810.

47. Snor, W., et al., *On the structure of anhydrous β-cyclodextrin.* Chemical Physics Letters, 2007. **441**(1–3): p. 159-162.

48. Sugita, Y. and Y. Okamoto, *Replica-exchange molecular dynamics method for protein folding.* Chemical Physics Letters, 1999. **314**(1–2): p. 141-151.

49. Hukushima, K. and K. Nemoto, *Exchange Monte Carlo Method and Application to Spin Glass Simulations.* Journal of the Physical Society of Japan, 1996. **65**(6): p. 1604-1608.

50. Case, D.A., et al., *{Amber 14}*. 2014.

51. Kirschner, K.N., et al., *GLYCAM06: A generalizable biomolecular force field. Carbohydrates.* Journal of Computational Chemistry, 2008. **29**(4): p. 622-655.

52. Tessier, M.B., et al., *Extension of the GLYCAM06 biomolecular force field to lipids, lipid bilayers and glycolipids.* Molecular Simulation, 2008. **34**(4): p. 349-364.

53. Khuntawee, W., et al., *Conformation study of ε-cyclodextrin: Replica exchange molecular dynamics simulations.* Carbohydrate Polymers, 2016. **141**: p. 99-105.

5. Outputs

5.1 การไปเสนอผลงาน การได้รับเชิญไปเป็นวิทยากร

1. T. Rungrotmongkol, Inclusion Complexation of Insoluble Compounds with Cyclodextrins, The 3rd International Conference on Computational Science and Engineering, Ho Chi Minh City, Vietnam, November 28-30, 2016 (*Invited speaker*)

2. T. Rungrotmongkol, Cyclodextrin: A Promising drug carrier for poorly water-soluble compounds, The First Materials Research Society of Thailand International Conference (MRS-Thailand 2017), Convention Center, The Empress Hotel, Chiang Mai, October 31 - November 3, 2017 *(invited speaker)*

3. T. Rungrotmongkol, Molecular calculations on the activity and development of anti-cancer agents, TRF-OHEC Annual Congress 2018 (TOAC 2018), The Regent Cha-am Beach Resort, January 10-12, 2018 *(poster presentation)*

4. T. Rungrotmongkol, Theoretical and Experimental Studies on the activity and development of anti-cancer agents, Pure and Applied Chemistry International Conference *(*PACCON*)*, International Convention Hall, Hat Yai, Songkhla, February *6-9*, 2018 *(oral presentation)*

5. T. Rungrotmongkol, Molecular modelling on biological systems, The 6th Biochemistry and Molecular Biology International Conference (6th BMB), The Rayong Resort, Rayong, June 20-22, 2018 (*invited speaker: Prof. M.R. Jisnuson Svasti-BMB Awardee*)

6. T. Rungrotmongkol, Biomolecular Structure and Dynamics of Proteins: A Computational Biology Approach, The 13rd International Symposium of the Protein Society of Thailand, Chulabhorn Research Institute, Thailand, August 7-9, 2018 (*invited speaker: Prof. M.R. Jisnuson Svasti Young Protein Scientist Awardee*)

7. T. Rungrotmongkol, Atomic-level insight into biological processes of molecular recognition, protein dynamics and catalytic origin of enzyme catalysis, Quantum International Frontiers 2018, Changsha, Hunan, P.R. China, October 17-21, 2018 *(Pedagogical lecture)*

8. P. Mahalapbutr, K. Sangpheak, T. Rungrotmongkol, Molecular Calculations on the Activity and Development of Anti-Cancer Agents, International Conference cum Workshop on Informatics Tools in Drug Discovery and Delivery (IT-DDD 2018), Punjabi University, Punjab, India, November 1-4, 2018. (*invited speaker*)

9. T. Rungrotmongkol, Molecular Calculations on the Activity and Development of Anti-Cancer Agents, TRF-OHEC Annual Congress 2019 (TOAC 2019), The Regent Cha-am Beach Resort, January 9-11, 2019 *(oral presentation)*

10. T. Rungrotmongkol, Mechanisms of drug action and mechanistic insights into enzyme catalysis, The 14th Pure and Applied Chemistry International Conference 2019 (PACCON 2019), Bangkok International Trade and Exhibition Center (BITEC), Bangkok, February 7-8, 2019 *(oral presentation)*

11. T. Rungrotmongkol, Biomolecular Structure and Function, Mechanisms of Drug Action, Source of Microbial Resistance and Mechanistic Insights into Enzyme Catalysis, The 6th NRCT-IFS-PERCH-CIC Workshops: ASEAN Research and Innovation Initiatives, Chiang Mai Grandview Hotel & Convention Center, Chiang Mai, February 19–24, 2019. *(poster presentation)*

12.

5.2 การเชื่อมโยงทางวิชาการกับนักวิชาการอื่น ๆทั้งในและต่างประเทศ

ภายในประเทศ

1. ผศ.ดร.วรินทร ชวศิริ *ภาควิชาเคมี* คณะวิทยาศาสตร์ จุฬาลงกรณ์มหาวิทยาลัย
2. ผศ.ดร.ปิยนุช วงศ์อนันต์ คณะแพทย์ศาสตร์ จุฬาลงกรณ์มหาวิทยาลัย
3. รศ.ดร.เกียรติทวี ชูวงศ์โกมล *ภาควิชาชีวเคมี* คณะวิทยาศาสตร์ มหาวิทยาลัยเกษตรศาสตร์
4. ผศ.ดร.นาวี กังวาลย์ ภาควิชาเคมี คณะวิทยาศาสตร์ มหาวิทยาลัยเชียงใหม่
5. ดร.ชมพูนุช รุ่งนิ่ม ศูนย์นาโนเทคโนโลยีแห่งชาติ *(National Nanotechnology Center: NANOTEC)*

ต่างประเทศ

1. Prof. Peter Wolschann, University of Vienna, Austria
2. Dr.Monika Mueller, University of Vienna, Austria
3. Assoc. Prof. Hisashi Okumura, Institute for Molecular Science, Japan
4. Prof. Seiji Mori, Ibaraki University, Japan

5.3 Publications

1. P. Mahalapbutr, P. Chusuth, N. Kungwan, W. Chavasiri, P. Wolschann, **T. Rungrotmongkol***. Molecular recognition of naphthoquinone-containing compounds against human DNA topoisomerase IIα ATPase domain: A molecular modeling study. Journal of Molecular Liquid, **2017**. 247: p. 374-385.
2. K. Sangpheak, M. Mueller, N. Darai, P. Wolschann, C. Suwattanasophon, R. Ruga, W. Chavasiri, S. Seetaha, K. Choowongkomon, N. Kungwan, C. Rungnim, **T. Rungrotmongkol***, Computational screening of chalcones acting against topoisomerase IIα and their cytotoxicity towards cancer cell lines, *Journal of Enzyme Inhibition and Medicinal Chemistry*, **2019**. 34 (1): p. 134-143.
3. P. Mahalapbutr, B. Nutho, P. Wolschann, N. Kungwan, **T. Rungrotmongkol***, Molecular Insights into Inclusion Complexes of Mansonone E and H Enantiomers with various β-cyclodextrins, Journal of Molecular Graphics and Modeling 2018, 79, 72-80.

4. K. Kerdpol, J. Kicuntod, P. Wolschann, S. Mori, C. Rungnim, M. Kunaseth, H. Okumura, N. Kungwan and **T. Rungrotmongkol***, Cavity Closure of 2-Hydroxypropyl-β-Cyclodextrin: Replica Exchange Molecular Dynamics Simulations. *Polymers*, **2019**. 11(1): p. 145.